

# Stability of Inhomogeneous Multi-Component Fermi Gases

D. Blume,<sup>1,2</sup> Seth T. Rittenhouse,<sup>3</sup> J. von Stecher,<sup>3</sup> and Chris H. Greene<sup>3</sup>

<sup>1</sup>*Department of Physics and Astronomy, Washington State University, Pullman, Washington 99164-2814*

<sup>2</sup>*JILA, University of Colorado, Boulder, CO 80309-0440*

<sup>3</sup>*Department of Physics and JILA, University of Colorado, Boulder, CO 80309-0440*

(Dated: February 4, 2008)

Two-component equal-mass Fermi gases, in which unlike atoms interact through a short-range two-body potential and like atoms do not interact, are stable even when the interspecies  $s$ -wave scattering length becomes infinitely large. Solving the many-body Schrödinger equation within a hyperspherical framework and by Monte Carlo techniques, this paper investigates how the properties of trapped two-component gases change if a third or fourth component are added. If all interspecies scattering lengths are equal and negative, our calculations suggest that both three- and four-component Fermi gases become unstable for a certain critical set of parameters. The relevant length scale associated with the collapse is set by the interspecies scattering length and we argue that the collapse is, similar to the collapse of an attractive trapped Bose gas, a many-body phenomenon. Furthermore, we consider a three-component Fermi gas in which two interspecies scattering lengths are negative while the other interspecies scattering length is zero. In this case, the stability of the Fermi system is predicted to depend appreciably on the range of the underlying two-body potential. We find parameter combinations for which the system appears to become unstable for a finite negative scattering length and parameter combinations for which the system appears to be made up of weakly-bound trimers that consist of one fermion of each species.

PACS numbers:

## I. INTRODUCTION

Over the past decade or so, the field of ultracold gases has seen tremendous breakthroughs. After reaching degeneracy in Bose [1, 2] and Fermi [3] gases, the realization of an atom laser [4, 5, 6], of the Mott-insulator transition [7], and of the conversion from an atomic to a molecular gas [8] followed. Many of the present-day studies take advantage of the tunability of the atom-atom scattering length in the vicinity of a so-called Fano-Feshbach resonance [9, 10]. As an external magnetic field is tuned through its resonance value, the sign of the scattering length changes [11, 12]. Exactly on resonance, the scattering length is infinitely large, allowing for the study of strongly-correlated systems. Experimentally, the speed of the magnetic field ramp can be changed, allowing adiabatic ramps, for example, and the ramp itself can be reversed. It is this versatility that made possible the experimental study of the BCS-BEC crossover, using ultracold atomic Fermi gases trapped in two different hyperfine states [13, 14].

Using present-day technology, the realization of degenerate multi-component atomic Fermi gases appears possible in principle. The occupation of more than two different hyperfine states of the same species requires, neglecting for the moment possible losses, only moderate changes of current set-ups. A particularly promising candidate appears to be  $^6\text{Li}$  [15], and the coexistence of three hyperfine states has already been demonstrated for  $^{40}\text{K}$  [16]. Alternatively, a number of groups are presently pursuing the simultaneous trapping of three different atomic species [17, 18]. In the former scenario, the atomic masses of all components are equal, whereas in the latter

scenario, the atomic masses of the different components differ. In either of these realizations of multi-component Fermi gases, all or some of the interspecies scattering lengths may be tunable thanks to the possible existence of magnetic or optical Fano-Feshbach resonances. This may open the possibility to experimentally investigate the stability and to study, provided an extended stable regime exists, the behaviors of multi-component Fermi gases as a function of the  $s$ -wave scattering length.

Using two different theoretical frameworks, this paper considers three- and four-component Fermi gases, and compares their behaviors with those of two-component Fermi gases. In particular, we ask how the stability of two-component Fermi gases changes when a third or fourth component are added. It is now well established that trapped two-component Fermi gases are stable even when the interspecies  $s$ -wave scattering length is negative and its magnitude is infinitely large [19, 20, 21, 22, 23]. The stability of inhomogeneous as well as of homogeneous two-component Fermi gases with attractive short-range interactions and arbitrary interspecies scattering length can be attributed to the Pauli exclusion principle (also referred to as Fermi pressure), which introduces effective repulsive intraspecies interactions that more than compensate the attractive interspecies interactions. In contrast, homogeneous Bose gases with negative scattering lengths are unstable; they can, however, be stabilized by an external confining potential as long as the product of the number of bosons and the  $s$ -wave scattering length is less negative than a certain critical value [24, 25, 26].

Section II introduces the Hamiltonian of trapped multi-component Fermi gases as well as a simple “counting argument” that turns out to be quite useful in understanding the stability of multi-component Fermi gases.

Section III investigates the stability of three- and four-component equal-mass Fermi gases within a hyperspherical framework, focussing on the large and small particle number limits. The physical picture emerging from the hyperspherical treatment is further investigated in Sec. IV, which solves the many-body Schrödinger equation for short-range interactions using Monte Carlo techniques. Finally, Sec. V summarizes and connects our results with those available in the literature [20, 27, 28, 29, 30, 31, 32, 33, 34, 35, 36, 37, 38, 39, 40].

## II. HAMILTONIAN AND GENERAL CONSIDERATIONS

The Hamiltonian  $H$  for an atomic Fermi gas with  $\chi$  components under external spherically symmetric harmonic confinement is given by

$$H = \sum_{\alpha=1}^{\chi} \sum_{i=1}^{N_{\alpha}} \left( -\frac{\hbar^2}{2m_{\alpha}} \nabla_{\vec{r}_{\alpha i}}^2 + \frac{1}{2} m_{\alpha} \omega_{\alpha}^2 r_{\alpha i}^2 \right) + \sum_{\alpha < \beta}^{\chi} \sum_{i=1}^{N_{\alpha}} \sum_{j=1}^{N_{\beta}} V_{\alpha\beta}(|\vec{r}_{\alpha i} - \vec{r}_{\beta j}|). \quad (1)$$

Here, the number of atoms of the  $\alpha$ th component is denoted by  $N_{\alpha}$ , and the total number of atoms is given by  $N$ ,  $N = \sum_{\alpha=1}^{\chi} N_{\alpha}$ . In Eq. (1),  $\vec{r}_{\alpha i}$  denotes the position vector of the  $i$ th atom of the  $\alpha$ th component, measured with respect to the center of the trap, and  $m_{\alpha}$  and  $\omega_{\alpha}$  respectively the atomic mass and the angular frequency of the  $\alpha$ th component. The potential  $V_{\alpha\beta}$  describes the interaction between an atom of the  $\alpha$ th and an atom of the  $\beta$ th component. This work considers a zero-range potential (see towards the end of this section and Sec. III) and a purely attractive short-range potential (see Sec. IV). In both cases, we characterize the strengths of the  $V_{\alpha\beta}$  by the  $s$ -wave scattering lengths  $a_{\alpha\beta}$ . We assume that the two-body interactions are independent of spin, implying that the number of atoms in each spin state is conserved. Throughout this work, like atoms are taken to be non-interacting, implying  $a_{\alpha\alpha} = 0$  for  $\alpha = 1, \dots, \chi$ .

In the most general case, the Hamiltonian given in Eq. (1) has  $\chi$  different  $m_{\alpha}$ ,  $\omega_{\alpha}$  and  $N_{\alpha}$  ( $\alpha = 1, \dots, \chi$ ), and  $\chi(\chi-1)/2$  different  $V_{\alpha\beta}$  ( $\alpha, \beta = 1, \dots, \chi$  and  $\alpha \neq \beta$ ), resulting in a tremendously large parameter space. To reduce the parameter space, we first consider the case where all  $m_{\alpha}$ , all  $\omega_{\alpha}$ , all  $N_{\alpha}$ , and all  $a_{\alpha\beta}$  ( $\alpha \neq \beta$ ) are equal. A four-component gas of this type could, e.g., be realized by equally populating and trapping the four spin states of a fermionic atom whose ground state has vanishing total electronic angular momentum  $J$  but a non-vanishing nuclear spin  $I$  of  $3/2$ . In this case, the scattering lengths between the different spin substates are equal and  $s$ -wave scattering between two atoms in the same spin substate are forbidden by symmetry.

Before solving the Schrödinger equation for the Hamiltonian given in Eq. (1), we present a simple counting

TABLE I: Number  $N_{att}$  of attractive interactions, number  $N_{rep}$  of effectively repulsive interactions and ratio  $N_{rep}/N_{att}$  for finite and infinite  $N$  for a  $\chi$ -component Fermi gas ( $\chi = 2$  through 4) in which all interspecies interactions are equal (or resonant).

	$\chi = 2$	$\chi = 3$	$\chi = 4$
$N_{att}$	$\frac{1}{4}N^2$	$\frac{1}{3}N^2$	$\frac{3}{8}N^2$
$N_{rep}$	$\frac{N}{2} \left( \frac{N}{2} - 1 \right)$	$\frac{N}{2} \left( \frac{N}{3} - 1 \right)$	$\frac{N}{2} \left( \frac{N}{4} - 1 \right)$
$N_{rep}/N_{att}$ ( $N$ finite)	$\frac{N-2}{N}$	$\frac{N-3}{2N}$	$\frac{N-4}{3N}$
$N_{rep}/N_{att}$ ( $N \rightarrow \infty$ )	1	$\frac{1}{2}$	$\frac{1}{3}$

analysis. The number  $N_{att}$  of attractive pair interactions  $V_{\alpha\beta}$ , where again  $\alpha \neq \beta$ , is given by

$$N_{att} = \frac{N^2}{2} \frac{\chi - 1}{\chi}, \quad (2)$$

and the number  $N_{rep}$  of effectively repulsive interactions, i.e., the number of like fermion pairs, by

$$N_{rep} = \frac{N}{2} \frac{N - \chi}{\chi}. \quad (3)$$

Table I summarizes the values of  $N_{att}$ ,  $N_{rep}$  and  $N_{rep}/N_{att}$  for  $\chi = 2, 3$  and 4. The ratio  $N_{rep}/N_{att}$  (reported in the fourth and fifth row of Table I for finite and infinite  $N$ , respectively) decreases with increasing  $\chi$  and approaches  $1/(\chi - 1)$  in the large  $N$  limit, indicating that the Fermi pressure becomes less important compared to the interspecies interactions as  $\chi$  increases. Another interesting scenario arises when each component is occupied by exactly one fermion, i.e., when  $\chi = N$ . In this case, no effectively repulsive interactions exist, i.e.,  $N_{rep}/N_{att} = 0$ , and the system's ground state is the same as that of the corresponding  $N$ -boson system. As pointed out already in the introduction, Bose gases with negative scattering length become unstable in the limit that the absolute value of the scattering length becomes large. This, together with the fact that two-component Fermi gases are stable for all scattering lengths, suggests that there exists a critical  $\chi$ -value beyond which multi-component Fermi gases with large negative interspecies scattering length are unstable. Sections III and IV show that  $\chi_{cr} = 3$ .

In addition to Fermi gases in which all interspecies interactions  $V_{\alpha\beta}$  ( $\alpha, \beta = 1, \dots, \chi$  and  $\alpha \neq \beta$ ) are equal, we consider the scenario in which only a subset of interspecies interactions are “turned on”. In particular, we consider  $\chi$ -component Fermi gases with  $\chi - 1$  equal and non-zero (or resonant)  $a_{\alpha\beta}$ . For the three-component system, we take  $a_{12} = a_{23}$  and  $a_{31} = 0$ . The number of attractive interactions is in this case by a factor of  $2/3$  smaller than in the case with three resonant interactions, thus increasing the ratio of  $N_{rep}/N_{att}$  from  $1/2$  to  $3/4$  in the large  $N$  limit. For the four-component system, two different “non-trivial” possibilities for turning on only  $\chi - 1$  interactions exist: (i)  $a_{12} = a_{13} = a_{14}$

and  $a_{23} = a_{34} = a_{24} = 0$ , and (ii)  $a_{12} = a_{23} = a_{34}$  and  $a_{13} = a_{14} = a_{24} = 0$  [the configuration  $a_{12} = a_{23} = a_{34}$  and  $a_{13} = a_{14} = a_{24} = 0$ , e.g., is equivalent to (i); the configuration  $a_{12} = a_{23} = a_{31}$  and  $a_{14} = a_{24} = a_{34} = 0$ , e.g., is trivial in the sense that it can be broken up into a three-component system with all resonant interactions and a single non-interacting component]. For the non-trivial configurations, the number of attractive interactions is half as large for the case of three resonant interactions as in the case of six resonant interactions, thus increasing the ratio of  $N_{rep}/N_{att}$  from  $1/3$  to  $2/3$  in the large  $N$  limit. This counting analysis indicates that the values of the ratio  $N_{rep}/N_{att}$  for large  $N$  for three- and four-component gases with  $\chi - 1$  resonant  $a_{\alpha\beta}$  are between those for two- and three-component Fermi gases with  $\chi(\chi - 1)/2$  resonant  $a_{\alpha\beta}$ . Thus, the question arises whether multi-component Fermi gases with  $\chi - 1$  resonant interactions are stable for all scattering lengths and  $N$  values, or whether they become unstable for a certain critical parameter combination.

To analyze the stability of Fermi gases quantitatively, one may attempt to describe the interspecies atom-atom interactions by a zero-range Fermi pseudopotential  $V_\delta(\vec{r})$  [41],

$$V_\delta(\vec{r}) = \frac{2\pi\hbar^2 a_s}{\mu} \delta(\vec{r}), \quad (4)$$

which is directly proportional to the  $s$ -wave scattering length  $a_s$ . Here,  $\mu$  denotes the reduced mass of the two interacting atoms. This pseudopotential has been employed successfully to predict many properties of dilute Bose gases. For example, the interaction potential given in Eq. (4) together with a Hartree wave function correctly predicts that trapped Bose gases with negative  $a_s$  become unstable if [24, 42]

$$(N - 1) \frac{a_s}{a_{ho}} \lesssim -0.575, \quad (5)$$

where  $a_{ho}$  denotes the oscillator length,  $a_{ho} = \sqrt{\hbar/(2\mu\omega)}$ . In general, the true atom-atom interaction can be replaced in the long-wavelength limit by the pseudopotential given in Eq. (4) provided the system is dilute, i.e., if  $n(0)|a_s|^3 \ll 1$ , where  $n(0)$  denotes the peak density. Assuming  $N$  is not too small, one finds that  $n(0)|a_s|^3$  is much smaller than one when  $(N - 1)a_s$  equals  $-0.575a_{ho}$ ; consequently, the pseudopotential predicts the instability of dilute Bose gases correctly.

Applied to two-component Fermi gases, the bare pseudopotential employed within a hyperspherical framework predicts that the system becomes unstable if [43]

$$k_F(0)a_s \lesssim -1.22, \quad (6)$$

where  $k_F(0)$  denotes the noninteracting Fermi wave vector at the trap center. (A mean-field analysis predicts a slightly more negative critical value of  $k_F(0)a_s \lesssim -\pi/2$  [44, 45, 46].) However, at the critical parameter combination  $k_F(0)a_s = -1.22$ , the diluteness criterion,

which can be written as  $(k_F(0)|a_s|)^3 \ll 1$  for fermions, is violated and the instability prediction, Eq. (6), cannot be trusted. Indeed, Eq. (6) disagrees with the experimental finding that two-component Fermi gases are stable [13, 14, 47, 48, 49, 50]. To resolve this disagreement, two independent studies recently introduced density-dependent “renormalization schemes” of the scattering length  $a_s$  entering into Eq. (4) [51, 52]. Using these “renormalization schemes”, the (modified) density-dependent pseudopotential can be applied to describe strongly-interacting Fermi gases and predicts, in agreement with experimental [13, 14, 47, 48, 49, 50] and other theoretical [19, 20, 21, 22, 53] works, that two-component Fermi gases are stable even in the strongly-interacting unitary regime. The fact that the Fermi pseudopotential has to be modified when applied to fermions was already suggested earlier (see, e.g., Refs. [44, 54]), and is well known in the nuclear physics community (see, e.g., Refs. [55, 56] and references therein).

The instability prediction given in Eq. (6) for two-component Fermi gases can be readily generalized to multi-component Fermi gases with  $\chi(\chi - 1)/2$  and with  $\chi - 1$  resonant interactions (in the case of  $\chi - 1$  resonant interactions, we consider the non-trivial scenario introduced above, in which none of the components can be separated off). The right hand side of Eq. (6) has to be multiplied by  $1/(\chi - 1)$  in the former case, and by  $\chi/[2(\chi - 1)]$  in the latter case. Since the diluteness criterion is fulfilled approximately in the all resonant case at the predicted collapse point [e.g.,  $(k_F(0)a_s)^3 \approx -0.23$  and  $-0.067$  for  $\chi = 3$  and  $4$ , respectively], the prediction that multi-component Fermi gases with all resonant interactions become unstable for a finite  $|a_s|$ , derived using the “bare” interaction given in Eq. (4), may in fact be correct. Sections III and IV confirm this. In the case with  $\chi - 1$  resonant interactions, the bare Fermi pseudopotential, Eq. (4), predicts that the collapse occurs at  $(k_F(0)a_s)^3 \approx -0.76$  and  $-0.54$  for  $\chi = 3$  and  $4$ , respectively. This suggests that the bare pseudopotential cannot be used and that the instability prediction derived using it may not be correct (see Sec. IV for a many-body analysis).

### III. HYPERSPHERICAL FRAMEWORK

#### A. $N$ -particle system

This section investigates the stability of three- and four-component Fermi gases within a hyperspherical framework [37, 43, 57, 58]. Throughout this section, we assume that all angular trapping frequencies are equal, i.e.,  $\omega_\alpha = \omega$  for  $\alpha = 1, \dots, \chi$ . To gain insight into the system’s behavior, we employ hyperspherical coordinates: the  $3N$  coordinates are divided into a hyperradius  $R$  and  $3N - 1$  hyperangles, collectively denoted by  $\Omega$  [59]. In the following, only the definition of the hyperradius  $R$ , which can be thought of as a measure of the size of the

system, is needed,

$$R = \left( \frac{1}{M} \sum_{\alpha=1}^{\chi} \sum_{i=1}^{N_{\alpha}} m_{\alpha} \vec{r}_{\alpha i}^2 \right)^{\frac{1}{2}}. \quad (7)$$

As before, the position vectors  $\vec{r}_{\alpha i}$  are measured with respect to the center of the trap. In Eq. (7),  $M$  denotes the total mass of the system, i.e.,  $M = \sum_{\alpha=1}^{\chi} \sum_{i=1}^{N_{\alpha}} m_{\alpha}$ . Using these coordinates, the many-body wave function  $\Psi(R, \Omega)$  can be expanded in terms of a set of  $\Omega$ -dependent channel functions  $\Phi_{\nu}(\Omega; R)$ , which depend parametrically on  $R$ , and  $R$ -dependent weight functions  $F_{\nu n}(R)$ ,

$$\Psi(R, \Omega) = \sum_{\nu n} R^{(1-3N)/2} F_{\nu n}(R) \Phi_{\nu}(\Omega; R). \quad (8)$$

In the adiabatic hyperspherical approximation [57, 60, 61, 62, 63], which neglects off-diagonal coupling elements and additionally restricts the sum in Eq. (8) to a single term, the solution of the many-body Schrödinger equation reduces to determining an  $R$ -dependent effective potential  $V_{\nu}(R)$ , which includes part of the kinetic energy as well as the effects of the two-body interactions, and then solving an effective one-dimensional radial Schrödinger equation in the hyperradius  $R$ ,

$$\left[ -\frac{\hbar^2}{2M} \frac{\partial^2}{\partial R^2} + V_{\nu}(R) + V_{\text{trap}}(R) \right] F_{\nu n}(R) = E_{\nu n} F_{\nu n}(R), \quad (9)$$

where

$$V_{\text{trap}}(R) = \frac{1}{2} M \omega^2 R^2. \quad (10)$$

In general, the calculation of the effective potentials  $V_{\nu}(R)$  is, at least for many-body systems, just as hard as solving the many-body Schrödinger equation itself. In certain circumstances, however, the effective potentials or their functional form can be obtained more easily.

For weakly-interacting dilute equal-mass two-component Fermi gases, e.g., the effective hyperradial potential  $V_0(R)$  consists of two parts [37, 43]: The first part, which is proportional to  $c_{kin}/R^2$ , arises from the kinetic energy operator, and the second part, which is proportional to  $c_{int}/R^3$ , accounts for the particle-particle interactions.  $c_{kin}$  is positive, and  $c_{int}$  is directly proportional to the  $s$ -wave scattering length  $a_s$  [43]. If  $|a_s|$  is sufficiently small ( $a_s < 0$ ), the small  $R$  region, where the attractive  $c_{int}/R^3$  term dominates over the repulsive  $c_{kin}/R^2$  term, is separated by a “barrier” from the  $R$  region where the repulsive  $c_{kin}/R^2$  term dominates over the attractive  $c_{int}/R^3$  term. This barrier prevents the Fermi gas from collapsing to a cluster-like many-body bound state, thus explaining the stability of weakly-interacting dilute equal-mass two-component Fermi gases (see also Ref. [51]).

Analytical expressions for  $V_{\nu}(R)$  for equal-mass two-component Fermi gases have also been obtained in the

strongly-interacting limit [37, 64]. For infinitely large interspecies scattering lengths  $a_{\alpha\beta}$  ( $\alpha \neq \beta$ ), the adiabatic approximation introduced above is— for a class of states that arise assuming boundary conditions consistent with contact interactions when the distance between each pair of particles goes to zero [64], referred to as universal states in the following— exact and the universal effective potentials  $V_{\nu}(R)$  are given by

$$V_{\nu}(R) = \frac{\hbar^2(1 + C_{\nu})}{2MR^2}. \quad (11)$$

In Eq. (11), the  $C_{\nu}$  denote  $R$ -independent constants that arise from the integration over the  $3N - 1$  hyperangles. The functional form given in Eq. (11) has also been derived by explicitly solving the many-body Schrödinger equation for a class of variational wave functions using hyperspherical coordinates [37]. Using dimensional arguments, Eq. (11) can be understood as follows: The term of  $V_{\nu}(R)$  that accounts for the particle-particle interactions has— because of the absence of any other length scale in the problem— to scale in the same way with  $R$  as the  $1/R^2$  term that accounts for the kinetic energy contribution. The total universal effective hyperradial potential curves at unitarity thus have a simple functional form:  $V_{\nu}(R)$  dominates at small  $R$  and approaches plus or minus infinity in the  $R \rightarrow 0$  limit, depending on whether the quantity  $1 + C_{\nu}$  is positive or negative, and  $V_{\text{trap}}(R)$  dominates at large  $R$ .

For a two-component unitary Fermi gas, a number of  $C_{\nu}$  values are known. For  $N \leq 6$ , selected  $C_{\nu}$  with  $\nu \leq 2$  have been obtained using a correlated Gaussian (CG) basis set expansion-type approach [65]. For  $N \leq 30$ , upper bounds for the  $C_0$  have been obtained by the FN-DMC method [65].

In the large  $N$  limit, the value of  $C_0$  for equal-mass two-component Fermi gases at unitarity can be related to the universal parameter  $\beta$  of the homogeneous system using the hyperspherical framework of Ref. [37] that employs a density-dependent scattering length [52], leading to  $C_0 = \beta$  [37]. Alternatively, this relationship can be derived by applying the local density approximation to the trapped system (see, e.g., Ref. [65]). It is generally believed that the most accurate value for  $\beta$  has been obtained by the FN-DMC method [22, 66],  $\beta = -0.58$ . Since  $1 + \beta > 0$ , the universal hyperradial potential curve  $V_0(R) + V_{\text{trap}}(R)$  for large  $N$  (shown by a solid line in Fig. 1 using  $\beta = -0.58$ ) is repulsive at small  $R$ , preventing the collapse of the two-component unitary Fermi gas towards cluster-like bound states. The hyperspherical potential curve picture reveals an intuitive way of understanding the stability of the energetically lowest-lying gas-like state of two-component unitary Fermi gases.

In Fig. 1, the hyperradial potential  $V(R)$  and the hyperradius  $R$  are scaled by  $E_{NI}$  and  $R_{NI}$ , respectively, where  $E_{NI}$  denotes the energy of the non-interacting  $\chi$ -component Fermi system and  $R_{NI}$  the square root of the expectation value of  $R^2$  calculated for the non-interacting  $\chi$ -component Fermi system, i.e.,  $R_{NI} =$

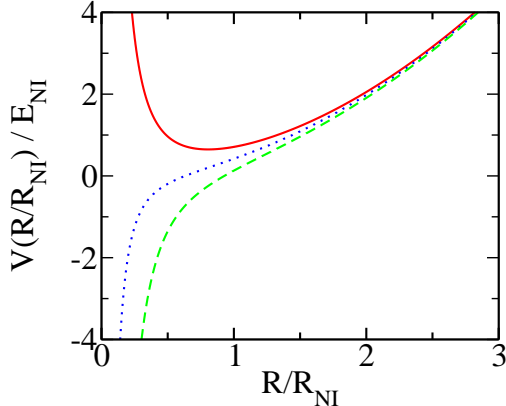


FIG. 1: (Color online) Hyperradial potential curve  $V_0(R) + V_{trap}(R)$  as a function of the hyperradius  $R$  for  $\chi = 2$  (solid line),  $\chi = 3$  (dotted line) and  $\chi = 4$  (dashed line) in the large  $N$  limit. All interactions between unlike atoms are characterized by an infinite scattering length, and the coefficient  $C_0$  is taken to be  $(\chi - 1)\beta$  with  $\beta = -0.58$ . Both length and energy are scaled by the corresponding values of the non-interacting system (see text).

$\sqrt{\langle R^2 \rangle_{NI}}$  [37, 43]. Using the virial theorem [64, 67],  $R_{NI}$  can be related to  $E_{NI}$ ,

$$R_{NI} = \sqrt{\frac{\hbar}{M\omega}} \sqrt{\frac{E_{NI}}{\hbar\omega}}. \quad (12)$$

In Fig. 1,  $E_{NI}$  and  $R_{NI}$  have been evaluated by writing  $E_{NI}$  as  $(\lambda + 3N/2)\hbar\omega$  and using the leading order of  $\lambda$  for large closed-shell systems,  $\lambda = (3N)^{4/3}/4$ . We note that the scaled quantity  $R/R_{NI}$  remains finite in the limit that  $N$  goes to infinity, allowing the thermodynamic limit to be taken.

For all-resonant three- and four-component gases at unitarity, the functional form given in Eq. (11) remains valid for universal states [37, 64]. For these systems, the values of  $C_\nu$  are not known (the only exception being the  $N = 3$  system [68, 69], see below). It has been argued [37], parametrizing  $V_{\alpha\beta}$  by a density-dependent zero-range two-body potential [52] and neglecting the existence of weakly-bound trimer or tetramer states, that the coefficient  $C_0$  is in the large  $N$  limit determined by the parameter  $\beta$  of the unitary two-component Fermi gas, i.e.,  $C_0 = (\chi - 1)\beta$ . Due to the lack of benchmark results for all-resonant three- and four-component Fermi gases, there is some ambiguity in how the simplest adaptation of the renormalization scheme, originally designed to describe the physics of two-component Fermi gases [52], is applied to three- and four-component Fermi gases, thus introducing some uncertainty about the exact values of  $C_0$  that describe unitary three- and four-component Fermi gases. Using  $C_0 = (\chi - 1)\beta$  and  $\beta = -0.58$  [22, 66],  $(1 + C_0)$  is negative for three- and four-component gases,  $(1 + C_0) = -0.16$  and  $(1 + C_0) = -0.74$  for  $\chi = 3$  and

4, respectively [70]. The resulting hyperradial potential curves  $V_0(R) + V_{trap}(R)$  are shown in Fig. 1 in the large  $N$  limit by dotted and dashed lines for  $\chi = 3$  and 4, respectively. The attractive small- $R$  behavior is due to the negative values of  $(1 + C_0)$ , and suggests that unitary three- and four-component Fermi gases with all resonant interactions are unstable. Note that the coefficient  $C_0$  and  $N_{att}/N_{rep}$  both scale as  $1 - \chi$  with  $\chi$ , reflecting the fact that  $V_0(R)$  is in part determined by the pair interactions.

Interestingly, both the bare pseudo-potential (see the discussion towards the end of Sec. II) and the density-dependent pseudo-potential (used in this section within the hyperspherical framework) predict that  $\chi$ -component Fermi gases,  $\chi > 2$ , with all resonant interactions become unstable for a finite value of the interspecies scattering length. The critical value predicted by the bare interaction is presumably not negative enough while that for the density-dependent interaction would presumably be too negative (we expect that the renormalization scheme originally developed for the two-component Fermi gas “over-renormalizes” the scattering length).

The analysis above can be extended to the case where only  $\chi - 1$  interspecies scattering lengths are infinite; as before, we focuss on what we defined in Sec. II as “non-trivial” scenarios. In the case of  $\chi - 1$  resonant interactions, the bare pseudopotential is expected to fail (see Sec. II). Using, just as above, density-dependent zero-range two-body interactions to describe the  $V_{\alpha\beta}$  with non-zero  $a_{\alpha\beta}$ , the coefficient  $C_0$  becomes in the large  $N$  limit  $\frac{2}{\chi}(\chi - 1)\beta$ ; just as in the all-resonant case,  $C_0$  scales with  $\chi$  in the same way as  $N_{att}/N_{rep}$ . Using  $\beta = -0.58$ ,  $(1 + C_0)$  is positive for  $\chi = 3$  and 4 (the corresponding potential curves are shown in Fig. 2); the repulsive small- $R$  behavior suggests that three- and four-component unitary Fermi gases with  $\chi - 1$  resonant interactions are stable. We note that the analysis in hyperspherical coordinates, which employs density-dependent interactions, has two short-comings: i) The derivation of the effective potential curves assumes the existence of a single length scale, the hyperradius  $R$ ; since some of the interspecies scattering length are zero while others are resonant, a more accurate description would presumably introduce an additional length scale and be based on a “hyperradial vector” as opposed to a single hyperradius. ii) The derivation neglects the possible existence of weakly-bound trimer (see the next section) or tetramer states, or said differently, the existence of non-universal states. Section IV B shows that the behaviors of multi-component Fermi gases with  $\chi > 2$  may differ depending on whether or not such states exist.

## B. Three-particle system

This section discusses the behaviors of three distinguishable fermions interacting through zero-range potentials with equal masses and equal trapping frequencies. For these systems, the effective hyperradial potential

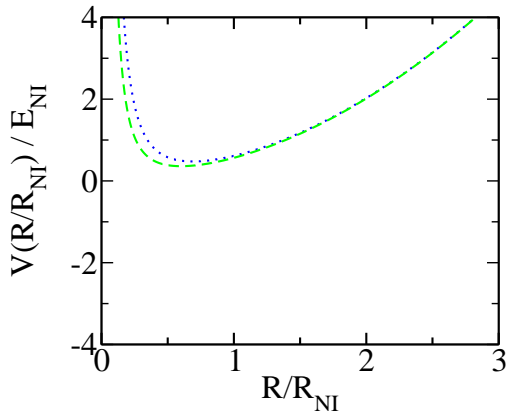


FIG. 2: (Color online) Hyperradial potential curve  $V_0(R) + V_{trap}(R)$  as a function of the hyperradius  $R$  for  $\chi = 3$  (dotted line) and  $\chi = 4$  (dashed line) in the large  $N$  limit for  $\chi - 1$  resonant interactions (the scattering lengths  $a_{1\beta}$ ,  $\beta = 2, \dots, \chi$ , are infinite and all other scattering lengths are zero). The coefficient  $C_0$  is taken to be  $\frac{2}{\chi}(\chi - 1)\beta$  with  $\beta = -0.58$ . Both length and energy are scaled by the corresponding values of the non-interacting system (see text). The plotting range of the axis is the same as in Fig. 1 for ease of comparison.

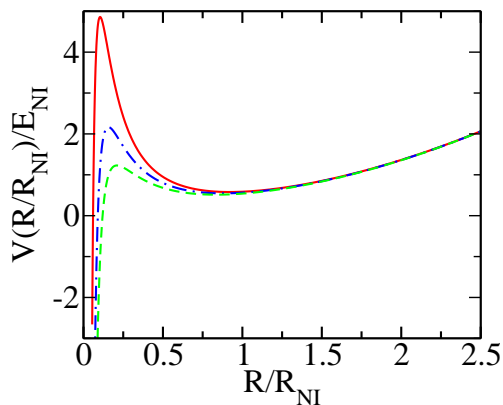


FIG. 3: (Color online) Solid, dash-dotted and dashed lines show the hyperradial potential curve  $V_0(R) + V_{trap}(R)$  as a function of the hyperradius  $R$ , scaled by  $R_{NI}$ , for three distinguishable fermions interacting through zero-range interactions with  $a_s = -0.1a_{ho}$ ,  $-0.15a_{ho}$  and  $-0.2a_{ho}$ , respectively. Note that  $R$  is defined without the center-of-mass motion, implying  $E_{NI} = 3\hbar\omega$ .

curves  $V_\nu(R)$  can be obtained analytically for any combination of scattering lengths  $a_{12}$ ,  $a_{23}$  and  $a_{31}$  [71, 72].

Figure 3 shows  $V_0(R) + V_{trap}(R)$  for the three-particle system as a function of  $R$  for three different negative scattering lengths  $a_s$ , i.e.,  $a_s = -0.1a_{ho}$ ,  $-0.15a_{ho}$  and  $-0.2a_{ho}$  (here,  $a_s = a_{\alpha\beta}$  with  $\alpha \neq \beta$ ) as a function of the hyperradius  $R$ . Throughout this section, the hyper-

radius  $R$  is defined without the center-of-mass motion and scaled by the hyperradius  $R_{NI}$  of the non-interacting system without the center-of-mass motion. For the discussion that follows, the difference between the hyperradius defined without the center-of-mass and that defined in Eq. (7) is irrelevant. For the scattering lengths shown, the hyperradial potentials show a barrier around  $R \approx 0.2R_{NI}$  (i.e.,  $R \approx 0.3a_{ho}$ ), which separates the large  $R$  region where gas-like states live from the small  $R$  region. As  $a_s$  becomes more negative, the barrier height decreases and moves to slightly larger  $R$  values. The critical scattering length  $a_c$  at which the barrier disappears ( $a_c \approx -0.39a_{ho}$ ) provides a first estimate for when the three-body system becomes “unstable” against the formation of tightly-bound trimer states with negative energy, assuming such states exist; the conditions for the existence of negative energy states are discussed below. A more accurate estimate would account for the zero-point energy of the quantum system, resulting in a somewhat less negative critical scattering length that is in fair agreement with the GP prediction given in Eq. (5) (see Ref. [57] for a discussion of the  $N$ -boson system). The lifetime of the gas-like three-body state can be estimated by calculating the tunneling rate through the potential barrier as a function of  $a_s$  [57]. When the barrier height is large compared to the energy of the non-interacting system (small  $|a_s|$ ), the lifetime of the gas-like trimer state is much larger than  $1/\omega$ ; in this case, the system can be considered stable (it is, in fact, metastable). The tunneling rate is appreciable only when the barrier height becomes comparable to the energy of the non-interacting system, i.e., when  $a_s$  approaches  $a_c$ .

To obtain the energy spectrum in the adiabatic approximation, we solve the one-dimensional radial Schrödinger equation [Eq. (9)]. To this end, we add a term  $V_{SR}(R)$  that is repulsive for  $R \lesssim R_c$  and negligibly small for  $R \gtrsim R_c$  to  $V_\nu(R)$ ,  $V_{SR}(R) = 2(1 - \sqrt{3}\tanh^2(R/R_c))/(2mR^2)$ .  $V_{SR}(R)$  cures the divergence of the  $V_\nu(R)$  at small  $R$ , which is related to the Thomas collapse [73]. When the barrier height is large compared to the energy of the non-interacting system and the short-range length scale  $R_c$  is chosen sufficiently small, this “ad-hoc” regularization should affect the eigenenergies of the gas-like states at most weakly. The eigenenergies of molecular-like states (states living in the small  $R$  region), however, should depend comparatively strongly on the particular value of  $R_c$ . Thus, some properties of the system are expected to be non-universal. Indeed, our calculations for different  $R_c$  show that the first state with negative energy appears when the scattering length  $a_s$  is approximately equal to  $-8.4R_c$ . For  $R_c = 0.001a_{ho}$ , e.g., the first negative energy state appears for  $a_s \approx -0.0084a_{ho}$ , a value much less negative than  $a_c$ . At this scattering length, the barrier height is large compared to the energy of the non-interacting system and the gas-like system is—because of the existence of a negative trimer state—metastable. If  $R_c$  is chosen so that the absolute value of the scattering length at which the first bound state appears is compa-

rable to or larger than  $|a_c|$ , then the gas-like state would be the true ground state of the system for  $|a_s| < |a_c|$ . For realistic dilute alkali gases with all-resonant interactions, we expect that three-body bound states appear for scattering lengths less negative than  $a_c$ ; consequently, trimer as well as larger three-component systems with  $a_s \gtrsim a_c$  are expected to be metastable. The picture developed here within the adiabatic approximation remains qualitatively valid if the coupling between channels is included.

In addition to the all-resonant three-particle system, we consider the trapped three-particle system with two resonant interactions ( $a_s = a_{12} = a_{23}$  and  $a_{31} = 0$ ). In this case, the hyperradial potential barrier disappears at a more negative scattering length than in the all-resonant case, i.e., at  $a_c \approx -1.00a_{ho}$ . An analysis of the tunneling probability suggests that the lifetime of the two-resonant system is, considering the same  $a_s$ , enhanced by a factor of about ten compared to the all-resonant system. A lifetime enhancement is expected since the ratio  $N_{att}/N_{rep}$  (see Sec. II) is smaller for the three-component system with two resonant interactions than for that with three resonant interactions.

Calculating the trimer energies in the adiabatic approximation, we find that the first three-body state with negative energy appears at  $a_s \approx -2500R_c$ . For example, a negative energy state appears for  $a_s \approx -2.5a_{ho}$  if  $R_c = 0.001a_{ho}$  and for  $a_s \approx -0.25a_{ho}$  if  $R_c = 0.0001a_{ho}$ . In the latter case, the disappearing of the hyperradial potential barrier is accompanied by a “collapse” of the metastable gas-like state to a cluster-like state. In the former case, in contrast, the disappearing of the hyperradial potential barrier is accompanied by the lowest-lying gas-like state evolving smoothly to a cluster-like state with negative energy. Although the short-range parameter  $R_c$  cannot be straightforwardly related to the parameters of typical atom-atom potentials, it seems plausible that realistic three-component Fermi systems with two resonant interactions could fall into either of the two categories discussed here. Section IV investigates the behaviors of three-component many-body systems and attempts to determine how the system’s behaviors depend on the range of the underlying finite-range two-body potential (this range can, roughly speaking, be connected with the short-range parameter  $R_c$ ).

We note that the negative scattering length  $a_s$  at which the first weakly-bound trimer state appears (assuming no deeply-bound states exist), can be estimated using the following “rule of thumb” [74, 75, 76]:  $|a_s| = R_c \exp(\pi/s_0)$ , where  $s_0$  is the coefficient that determines the energy spectrum of the lowest hyperradial potential curve at unitarity ( $s_0 = 1.006$  for  $a_s = a_{12} = a_{23} = a_{31}$ , and  $s_0 = 0.413$  for  $a_s = a_{12} = a_{23}$  and  $a_{31} = 0$  [68]). This rule of thumb predicts a negative scattering length at which the first weakly-bound trimer state appears of  $-23R_c$  and  $-2000R_c$  for three and two resonant interactions, respectively. These values are to be compared with  $-8.4R_c$  and  $-2500R_c$  found numerically (see above).

## IV. MONTE CARLO TREATMENT

This section discusses the solutions of the many-body Schrödinger equation for the Hamiltonian given in Eq. (1) obtained by Monte Carlo techniques as a function of the scattering length. Section IV A introduces the VMC and FN-DMC methods, and Sec. IV B presents our results.

### A. Variational and fixed-node diffusion Monte Carlo method

Using the VMC and FN-DMC methods [77], we determine solutions of the many-body Schrödinger equation for two different purely attractive short-range model potentials  $V_{\alpha\beta}$ : a square well interaction potential  $V_{\alpha\beta}^{SW}$ ,

$$V_{\alpha\beta}^{SW}(r) = \begin{cases} -V_{\alpha\beta,0} & \text{for } r < R_{\alpha\beta,0} \\ 0 & \text{for } r > R_{\alpha\beta,0}, \end{cases} \quad (13)$$

and a Gaussian interaction potential  $V_{\alpha\beta}^G$ ,

$$V_{\alpha\beta}^G(r) = -V_{\alpha\beta,0} \exp\left(-\frac{r^2}{2R_{\alpha\beta,0}^2}\right). \quad (14)$$

Both potentials depend on a depth  $V_{\alpha\beta,0}$ ,  $V_{\alpha\beta,0} \geq 0$ , and a range  $R_{\alpha\beta,0}$ . In our calculations, we set all  $R_{\alpha\beta,0}$  to the same value,  $R_{\alpha\beta,0} \ll a_{ho}$ , and adjust the depths  $V_{\alpha\beta,0}$  until the  $s$ -wave scattering lengths  $a_{\alpha\beta}$  assume the desired values. In Sec. IV B,  $V_{\alpha\beta,0}$  and  $R_{\alpha\beta,0}$  are chosen so that the potential  $V_{\alpha\beta}$  supports no two-body  $s$ -wave bound state and so that  $a_{\alpha\beta} \leq 0$ . The use of two different functional forms for the interaction potentials  $V_{\alpha\beta}$  allows for exploring the dependence of the results on the details of the short-range physics.

We now discuss how the solutions of the many-body Schrödinger equation are obtained by the variational Monte Carlo method. The functional form of the variational wave function  $\psi_T$  is chosen on physical grounds (see below), and  $\psi_T$  is parametrized in terms of a set of parameters  $\vec{p}$ , which are optimized so as to minimize the energy expectation value  $E(\vec{p})$  [77],

$$E(\vec{p}) = \frac{\langle \psi_T(\vec{p}) | H | \psi_T(\vec{p}) \rangle}{\langle \psi_T(\vec{p}) | \psi_T(\vec{p}) \rangle}. \quad (15)$$

Since  $\psi_T$  depends in general on the  $3N$  coordinates of the system, the integration on the right hand side of Eq. (15) is high-dimensional; this implies that standard techniques such as the Simpson rule [78], which scale, roughly speaking, exponentially with the number of degrees of freedom cannot be used for its evaluation. Instead, we evaluate the high-dimensional integral by Monte Carlo techniques using standard Metropolis sampling [79]. The stochastic evaluation of the integral introduces a statistical uncertainty, which can be reduced by increasing the number of samples  $K$  included in the evaluation of the expectation value (the errorbar decreases as  $1/\sqrt{K}$  with



increasing  $K$ ). We denote the energy expectation value obtained by the VMC method by  $E_{VMC}$ .

The variational wave function  $\psi_T$  for multi-component Fermi gases is written as (see Refs. [21, 22, 53, 65, 80, 81, 82] for Monte Carlo studies of two-component systems and Ref. [35] for a Monte Carlo study of three-component systems)

$$\psi_T = \prod_{\alpha < \beta} \prod_{i=1}^{\chi} \prod_{j=1}^{N_\beta} f_{\alpha\beta}(|\vec{r}_{\alpha i} - \vec{r}_{\beta j}|) \times \prod_{\alpha=1}^{\chi} \prod_{i=1}^{N_\alpha} \varphi_\alpha(\vec{r}_{\alpha i}) \times \prod_{\alpha=1}^{\chi} \mathcal{A}(\phi_1(\vec{r}_{\alpha 1}), \dots, \phi_{N_\alpha}(\vec{r}_{\alpha N_\alpha})), \quad (16)$$

where  $\mathcal{A}$  denotes the anti-symmetrizer and  $f_{\alpha\beta}$ ,  $\varphi_\alpha$  and  $\phi_i$  denote two- or one-body functions whose functional form is discussed in detail in the following.

The  $f_{\alpha\beta}$  denote two-body correlation factors. For small  $r$ ,  $f_{\alpha\beta}$  coincides with the zero-energy scattering wave function for two particles interacting through  $V_{\alpha\beta}$ . Beyond some matching value  $R_{\alpha\beta,m}$ , which is treated as a variational parameter,  $f_{\alpha\beta}$  is taken to be  $c_{\alpha\beta,1} + c_{\alpha\beta,2} \exp(-c_{\alpha\beta}r)$ , where  $c_{\alpha\beta}$  denotes a variational parameter and  $c_{\alpha\beta,1}$  and  $c_{\alpha\beta,2}$  are determined by the condition that  $f_{\alpha\beta}$  and its derivative are continuous at  $r = R_{\alpha\beta,m}$ . The  $R_{\alpha\beta,m}$  and  $c_{\alpha\beta}$  are optimized under the constraint that  $f_{\alpha\beta} \geq 0$  for all  $r$ .

The  $\varphi_\alpha$  denote Gaussian orbitals with widths  $b_\alpha$ ,  $\varphi_\alpha(\vec{r}) = \exp(-r^2/(2b_\alpha^2))$ . The parameters  $b_\alpha$  control the size of the Fermi cloud, and are optimized variationally. In the non-interacting case,  $b_\alpha = a_{ho}$ . For  $a_{\alpha\beta} < 0$ , the system becomes more compact due to the attractive interactions, resulting in a smaller optimal value of  $b_\alpha$ . If all  $m_\alpha$  and all  $b_\alpha$  are the same, i.e.,  $m_\alpha = m$  and  $b_\alpha = b$ , then the product  $\prod_{\alpha=1}^{\chi} \prod_{i=1}^{N_\alpha} \varphi_\alpha(\vec{r}_{\alpha i})$  reduces to  $\exp(-NR^2/(2b^2))$  and the variational parameter  $b$  is proportional to the mean hyperradius of the variational wave function.

The  $\phi_i(\vec{r})$  are given by  $H_{n_x}(x)H_{n_y}(y)H_{n_z}(z)$ , where  $(n_x, n_y, n_z) = (0, 0, 0)$  for  $i = 1$ ,  $(n_x, n_y, n_z) = (1, 0, 0)$  for  $i = 2$ ,  $(n_x, n_y, n_z) = (0, 1, 0)$  for  $i = 3$  and so on, and the  $H_n$  denote Hermite polynomials of degree  $n$ .

The anti-symmetry and nodal surface of  $\psi_T$  are determined by the  $\chi$  Slater determinants [second line of Eq. (16)], which contain the one-body functions  $\phi_i$ . The nodal surface of  $\psi_T$  coincides with that of the non-interacting multi-component Fermi gas. For small  $|a_{\alpha\beta}|$ ,  $a_{\alpha\beta} < 0$ , this is expected to be a very good approximation. It has been shown that the nodal surface used here also provides reasonably tight bounds for the energies of trapped two-component gases [65, 81, 82] all the way to unitarity. Whether this holds true for multi-component Fermi gases with  $\chi > 2$  should be addressed in more detail in follow-up work. Note that the guiding function  $\psi_T$  used throughout this work does not build in any “pairing physics” from the outset (see Sec. V for further discussion). The product  $\phi_\alpha(\vec{r})\varphi_i(\vec{r})$ ,  $i = 1, \dots, N_\alpha$ , with  $b_\alpha = a_{ho}$  coincides with the  $i$ th (non-normalized) single-

particle harmonic oscillator wave function. We choose to write  $\psi_T$  in terms of the product  $\phi_\alpha\varphi_i$  instead of the harmonic oscillator functions themselves, because this allows the widths  $b_\alpha$  of the Gaussians to be varied without changing the nodal surface of  $\psi_T$ .

In addition to the VMC method, we apply the FN-DMC method [77, 83]. The FN-DMC method uses the variational wave function  $\psi_T$  as a so-called guiding function and determines the energy of a state whose nodal surface is identical to that of  $\psi_T$ . It can be shown that the FN-DMC energy provides an upper bound to the lowest eigenenergy of the eigenstate that has the same symmetry as  $\psi_T$  [83]. If the nodal surface of  $\psi_T$  coincides with that of the true eigenfunction, then the FN-DMC method results, within the statistical uncertainty, in the exact eigenenergy. In general, the quality of the FN-DMC energy depends crucially on the construction of the nodal surface of  $\psi_T$ . As in the VMC method, expectation values calculated by the FN-DMC method have a statistical uncertainty, which can be reduced by increasing the computational efforts.

## B. Monte Carlo results

We first consider three- and four-component Fermi gases with one atom per component and equal masses and trapping frequencies. If all interspecies scattering lengths are equal, these Fermi gases are described by the same Hamiltonian as the corresponding Bose gas and the system should become unstable towards the formation of negative energy states, characterized by small interparticle distances, when the inequality given in Eq. (5) is fulfilled. For  $N = 3$  and 4, this implies critical scattering lengths of  $a_s \approx -0.29a_{ho}$  and  $-0.19a_{ho}$ , respectively.

To investigate how this instability or collapse arises within the many-body Monte Carlo framework, we perform DMC calculations for the three- and four-particle systems interacting through a square well potential with  $R_0 = 0.01a_{ho}$  (the subscripts  $\alpha$  and  $\beta$  of  $R_{\alpha\beta,0}$  have been dropped for notational convenience). The depth is chosen so that  $a_s$  takes the desired value and so that the potential supports no two-body bound states. For small  $|a_s|$ , the DMC method results in energies that agree very well with the mean-field Gross-Pitaevskii (GP) energy for both  $N = 3$  and 4. As  $a_s$  becomes more negative (of the order of  $-0.06a_{ho}$  [84]), the DMC walkers sample at first exclusively positive energy configurations; after a certain propagation time some walkers sample configurations with negative energy that correspond to tightly-bound states. The existence of tightly-bound three-body states, which depend on the details of the underlying two-body potential, for scattering lengths  $a_s$  that are less negative than the critical scattering lengths determined at the mean-field level or within the hyperspherical framework was already pointed out in Sec. III B. Our calculations here show that the DMC algorithm “sees” these three-body bound states (as well as four-body bound



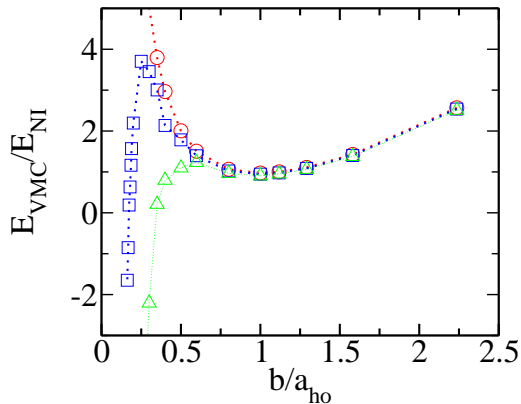


FIG. 4: (Color online) Circles, squares and triangles show the variational energy  $E_{VMC}$  for  $N = 3$  atoms interacting through a square well potential (range  $R_0 = 0.01a_{ho}$ ) with  $a_s = -0.05a_{ho}$ ,  $-0.1a_{ho}$  and  $-0.15a_{ho}$ , respectively, as a function of the variational parameter  $b$  [see the discussion following Eq. (16)].  $E_{VMC}$  is scaled by the energy  $E_{NI}$  of the non-interacting system,  $E_{NI} = 4.5\hbar\omega$ . Dotted lines connect data points for ease of viewing.

states) if the simulation time is sufficiently long and  $|a_s|$  is sufficiently large. If  $|a_s|$  is not too large, the DMC algorithm does—if the initial walker configurations correspond to gas-like states—not “know” about the tightly-bound states with negative energy.

To gain further insight, we treat the  $N = 3$  system by the VMC method. For a given  $a_s$ , we fix the variational parameters  $R_m$  and  $c$  (their exact values are not important for the discussion that follows) and vary  $b$  (we drop the subscripts  $\alpha$  and  $\beta$  of  $R_{\alpha\beta,m}$  and  $c_{\alpha\beta}$ , and the subscript  $\alpha$  of  $b_\alpha$ ). Circles, squares and triangles in Fig. 4 show the variational energy  $E_{VMC}$  for  $N = 3$  as a function of  $b$  for  $a_s = -0.05a_{ho}$ ,  $-0.1a_{ho}$  and  $-0.15a_{ho}$ , respectively. For  $a_s = -0.05a_{ho}$ ,  $E_{VMC}$  increases if the Gaussian width  $b$  is larger than about  $a_{ho}$  (the system expands compared to its optimal size, thereby reducing the attraction felt between the atoms) and if  $b$  is smaller than about  $a_{ho}$  (the system shrinks compared to its optimal size, thereby increasing the kinetic energy). For  $a_s = -0.1a_{ho}$  and  $-0.15a_{ho}$  (squares and triangles in Fig. 4), the variational energy assumes a local minimum at  $b \approx a_{ho}$ , shows a local maximum at  $b \approx 0.25a_{ho}$  for  $a_s = -0.1a_{ho}$  and at  $b \approx 0.5a_{ho}$  for  $a_s = -0.15a_{ho}$ , and becomes negative for yet smaller  $b$ . We refer to the local maximum as an “energy barrier” that separates the local minimum at  $b \approx a_{ho}$  from a global minimum that exists at smaller  $b$  values. Finally, for more negative scattering lengths (not shown in Fig. 4) no energy barrier exists for the variational wave functions considered.

The energy barrier discussed here for small  $s$ -wave interacting Bose gases also exists in three-dimensional dipolar Bose gases [85] and one-dimensional Bose

gases [86] (the second part of the Appendix in Ref. [85] provides a detailed discussion). As in those earlier studies, we interpret the existence of the energy barrier as an indication that the Hilbert space is divided into two nearly orthogonal spaces if  $a_s$  is quite a bit less negative than the critical scattering length predicted at the mean-field level: Gas-like states live in one region of the Hilbert space, and cluster-like bound states in the other. While this reasoning leads to an intuitive understanding of the stability and decay of Bose gases with negative scattering length, the question arises why the energy barrier disappears for scattering lengths  $a_s$  that are notably less negative than the critical scattering length predicted by the GP equation. We believe that this is due to the existence of tightly-bound states with negative energy. If  $|a_s|$  is sufficiently large, the overlap of the variational wave function with eigen functions of cluster-like bound states increases with decreasing  $b$ . For non-vanishing overlap,  $E_{VMC}$  provides a rather poor upper bound to the true ground state energy of the system and not an upper bound to the energetically lowest-lying gas-like state. This implies that our VMC calculations do not allow for a reliable determination of the critical scattering length. Instead, they indicate that the existence of the energy barrier gives rise to the stability of the gas-like state and that the disappearing of the energy barrier qualitatively explains how the instability of Bose gases and multi-component Fermi gases with one atom per component arises when  $a_s$  becomes too negative.

We note that the picture developed here based on our VMC and DMC calculations is closely related to the analysis based on the hyperspherical formulation presented in Sec. III and in Refs. [37, 57, 87, 88]. In the VMC calculations, the role of the hyperradius  $R$  is played by the Gaussian width  $b$  [see discussion following Eq. (16)]. Furthermore, variational mean-field calculations have been interpreted in much the same way [89, 90].

We now investigate the behaviors of multi-component Fermi gases with more than one atom per component for which all interspecies scattering lengths  $a_{\alpha\beta}$  with  $\alpha \neq \beta$  are resonant; as before, we set  $a_{\alpha\beta} = a_s$ . We first solve the many-body Schrödinger equation for a square well potential with range  $R_{\alpha\beta,0} = 0.01a_{ho}$  by the FN-DMC method. Circles in Fig. 5 show the FN-DMC energy for a four-component Fermi gas with four atoms per component (this corresponds to a closed shell) as a function of the  $s$ -wave scattering length  $a_s$ . The energy decreases approximately linearly with decreasing  $a_s$ , suggesting that this weakly-interacting system can be described to a good approximation perturbatively. Assuming zero-range interactions with scattering lengths  $a_s$  and treating the system within first order perturbation theory, we find  $E \approx 36\hbar\omega + ca_s/a_{ho}$ , where  $c = 93\hbar\omega/\sqrt{2\pi}$ , for  $N = 16$ . This perturbatively calculated energy (solid line in Fig. 5) describes the FN-DMC energies (circles) very well. By additionally treating the  $N = 17$  fermion system with  $N_1 = 5$  and  $N_2 = N_3 = N_4 = 4$  (squares in Fig. 5), we find that the chemical potential decreases,

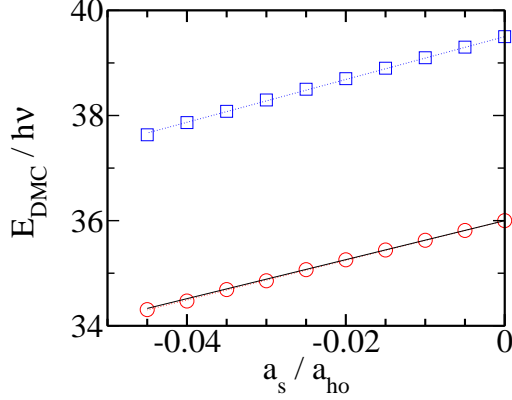


FIG. 5: (Color online) Circles and squares show the FN-DMC energy  $E_{DMC}$  for a four-component Fermi gas with  $N = 16$  and  $17$  atoms, respectively, interacting through a square well potential with range  $R_0 = 0.01a_{ho}$  as a function of the interspecies scattering length  $a_s$  (all interspecies scattering lengths are equal). While the  $N = 16$  system has four atoms per component, the  $N = 17$  system has one component with five atoms and three components with four atoms. Dotted lines show a linear fit to the FN-DMC energies: The slope is  $37.7\hbar\omega/a_{ho}$  for  $N = 16$  and  $40.7\hbar\omega/a_{ho}$  for  $N = 17$ . For comparison, the solid line shows the energy for  $N = 16$  calculated within first order perturbation theory,  $E = 36\hbar\omega + ca_s/a_{ho}$  with  $c \approx 37.1\hbar\omega$ .

just as the energy, approximately linearly with increasing  $|a_s|$ . For scattering lengths more negative than about  $-0.045a_{ho}$  [84], the DMC walkers sample—just as in the case of the small Bose systems—negative energy configurations. We find that the three-component Fermi gas with  $N = 12$  behaves similarly. At the FN-DMC level, the instability of multi-component Fermi gases is accompanied by the existence of cluster-like states with negative energy. To investigate whether these cluster-like states “live” for sufficiently small  $|a_s|$ , as in the case of Bose gases, in a Hilbert space that is approximately orthogonal to the Hilbert space where the gas-like states live, we perform a series of VMC calculations.

Circles and squares in Fig. 6 show the variational energy  $E_{VMC}$  for the three-component Fermi system with  $N = 12$  as a function of  $b$  for  $a_s = -0.05a_{ho}$  and  $-0.1a_{ho}$ , respectively (as before,  $b = b_\alpha$  and  $a_s = a_{\alpha\beta}$  where  $\alpha \neq \beta$ ). The lowest variational energy for  $a_s = -0.05a_{ho}$  is obtained for  $b \approx a_{ho}$ ,  $E_{VMC} = 26.09(4)\hbar\omega$ . The FN-DMC energy for this interspecies scattering length,  $E_{DMC} = 26.08(4)\hbar\omega$ , agrees with  $E_{VMC}$  within error bars, indicating that our variational wave function—assuming the nodal surface is adequate—captures the key physics of the system. For comparison, circles and squares in Fig. 7 show the variational energy  $E_{VMC}$  for the four-component Fermi system with  $N = 16$  as a function of  $b$  for  $a_s = -0.05a_{ho}$  and  $-0.07a_{ho}$ , respectively. A comparison of Figs. 6 and 7 shows that the overall behav-

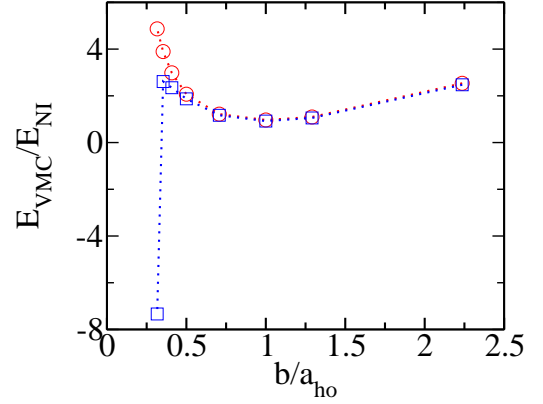


FIG. 6: (Color online) Circles and squares show the variational energy  $E_{VMC}$  for a three-component Fermi gas with  $N = 12$  atoms interacting through a square well potential (range  $R_0 = 0.01a_{ho}$ ) with  $a_s = -0.05a_{ho}$  and  $-0.1a_{ho}$  (all interspecies scattering lengths are equal), respectively, as a function of the variational parameter  $b$ .  $E_{VMC}$  is scaled by the energy  $E_{NI}$  of the non-interacting system,  $E_{NI} = 27\hbar\omega$ . Dotted lines connect data points for ease of viewing.

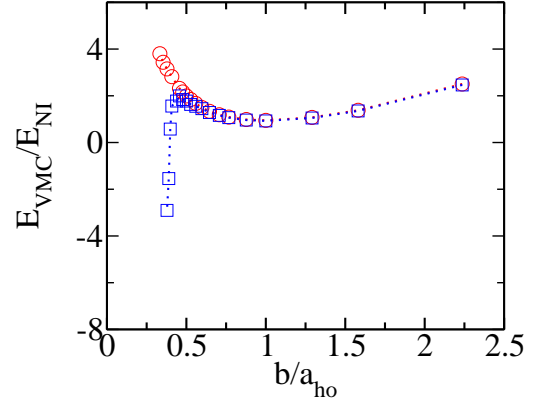


FIG. 7: (Color online) Circles and squares show the variational energy  $E_{VMC}$  for a four-component Fermi gas with  $N = 16$  atoms interacting through a square well potential (range  $R_0 = 0.01a_{ho}$ ) with  $a_s = -0.05a_{ho}$  and  $-0.07a_{ho}$ , respectively, as a function of the variational parameter  $b$ .  $E_{VMC}$  is scaled by the energy  $E_{NI}$  of the non-interacting system,  $E_{NI} = 36\hbar\omega$ . Dotted lines connect data points for ease of viewing.

ior of the three- and four-component systems is very similar, and resembles that discussed above for Bose gases: For small  $|a_s|$ ,  $E_{VMC}$  increases if the Gaussian width  $b$  is larger than about  $a_{ho}$  and if  $b$  is smaller than about  $a_{ho}$ . For somewhat more negative interspecies scattering lengths  $a_s$ ,  $E_{VMC}$  shows a local minimum at  $b \approx a_{ho}$  and a local maximum at  $b \approx 0.3a_{ho}$ , and  $E_{VMC}$  becomes neg-

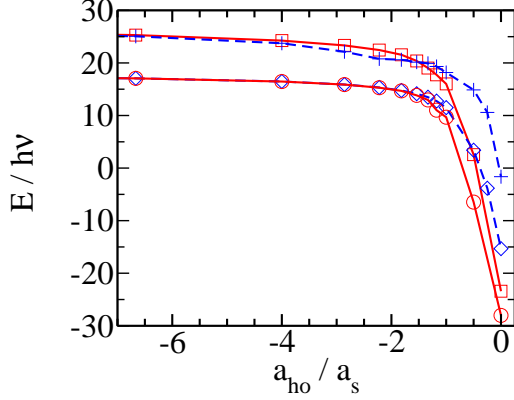


FIG. 8: (Color online) Energies for a three-component Fermi system as a function of  $a_{ho}/a_s$  for two resonant interactions. Circles and diamonds show the energy of the three-particle system, multiplied by a factor of four, interacting through a square well potential with range  $0.01a_{ho}$  and a Gaussian potential with range  $0.007a_{ho}$ , respectively; the energies for the square well potential are calculated by the FN-DMC approach and those for the Gaussian potential by the CG approach. Squares and pluses show the FN-DMC energies for  $N = 12$  for a square well potential with range  $0.01a_{ho}$  and a Gaussian potential with range  $0.007a_{ho}$ , respectively. Solid and dashed lines connect data points for ease of viewing.

ative for yet smaller  $b$ . For more negative  $a_s$  (not shown in Figs. 6 and 7), the energy barrier disappears. We note that the variational energies for  $b$  values of the order of  $0.3a_{ho}$  to  $0.6a_{ho}$  and  $a_s \lesssim -0.05a_{ho}$  show large fluctuations. For these systems, configurations with rather different “geometries”, and hence with rather different potential and kinetic energies, are being sampled, leading to non-Gaussian distributed energy expectation values. This behavior is a consequence of the fact that the variational wave function does not provide a good description of the true eigenfunction.

Our MC results for multi-component Fermi gases with all resonant interactions and  $\chi > 2$  support the physical picture developed in Sec. III within the hyperspherical framework about how the instability or “implosion” of the system arises. Furthermore, the VMC and FN-DMC results suggest that the stability and decay of multi-component Fermi gases can be attributed to the same mechanisms as the stability and decay of Bose gases. At the VMC level, the energy barrier arises on length scales that are comparable to  $|a_s|$  but much larger than the range of the two-body potential. This suggests that the onset of the instability is determined by the value of the scattering length as opposed to the details of the underlying two-body potential, assuming the range of the underlying two-body potential is sufficiently small (see also the discussion in Sec. III B).

We now discuss the behavior of three-component Fermi gases with equal masses and equal trapping frequencies in

which two interspecies scattering lengths, denoted in the following by  $a_s$ , are resonant and the third interspecies scattering length is zero. As before, the depths of the two-body potentials are adjusted so that the scattering lengths take the desired value and so that the two-body potentials support no two-body bound state (for  $a_{\alpha\beta} = 0$ , the depth is set to zero).

Motivated by the discussion presented in Sec. III B for the three-particle system we first consider two-body potentials with very small range. The trimer system interacting through a square well potential with  $R_0 = 0.001a_{ho}$  supports a state with negative energy for scattering lengths that are much less negative than the critical scattering length of  $a_c \approx -1a_{ho}$  predicted for  $N = 3$  (see Sec. III B). Thus, we expect the stability behavior of the three-component many-fermion system with two resonant interactions interacting through square well potentials with range  $R_0 = 0.001a_{ho}$  to be similar to that of the all-resonant system discussed above. Indeed, we find that the FN-DMC calculations for the  $N = 12$  system appear stable for small  $|a_s|$ , including a region of scattering lengths where the three-particle system supports negative energy states, but show instabilities for larger  $|a_s|$  ( $|a_s| < |a_c|$ ). The VMC energy is minimal for  $b \approx a_{ho}$  and increases for smaller and larger  $b$  values. Somewhat surprisingly, our VMC calculations do not indicate the existence of an energy minimum for small  $R$  values when  $a_s$  is close to  $a_c$ . This is different from the all-resonant systems and can possibly be attributed to the variational wave functions employed (for very small  $R_0$ , a more flexible functional form may be needed to obtain an energy minimum at small  $R$ ). We find similar results for the four-component system with three resonant interactions for which  $a_{1\beta} = a_s$  and  $a_{\alpha\beta} = 0$  otherwise (we did not perform Monte Carlo calculations for the second non-trivial configuration with  $\chi - 1$  resonant interactions, for which  $a_s = a_{12} = a_{23} = a_{34}$  and  $a_{\alpha\beta} = 0$  otherwise). Our FN-DMC results for multi-component Fermi gases with  $\chi - 1$  resonant interactions ( $\chi > 2$ ) and very small  $R_0$  suggest that these systems become unstable for a certain critical negative scattering length. In analogy to the Bose system, this seems to suggest that multi-component Fermi gases with very small  $R_0$  are stable for scattering lengths less negative than  $a_c$  and become mechanically unstable for scattering lengths more negative than  $a_c$ .

Next, we consider three-component Fermi gases interacting through two-body potentials with a somewhat larger range with  $a_s = a_{12} = a_{23}$  and  $a_{31} = 0$ . Figure 8 shows the energy for the three-particle system, multiplied by a factor of four, as a function of  $a_{ho}/a_s$  for the square well potential with  $R_0 = 0.01a_{ho}$  (circles) and the Gaussian potential with  $R_0 = 0.007a_{ho}$  (diamonds). The  $N = 3$  energies for the Gaussian potential are calculated by the CG approach [52, 65, 82, 91] (this approach is free of any assumptions, and its accuracy can be improved systematically) and those for the square well potential by the FN-DMC approach. For small  $|a_s|$ , the energies for the two different interaction potentials agree quite well

TABLE II: Summary of our stability analysis: In the large  $|a_s|$  limit, trapped  $\chi$ -component Fermi gases are predicted to be either stable (“S”) or unstable (“U”), or to form a (possibly stable) gas of trimers (“S(?)GT”). The predictions are based on the hyperspherical treatment, which employs the bare and the density-dependent pseudo-potential, and a many-body Monte Carlo framework. <sup>(1)</sup>Only systems with  $a_s = a_{12} = a_{13} = a_{14}$  and  $a_{\alpha\beta} = 0$  otherwise with very small two-body range were investigated.

$\chi$	hyperspherical (“bare” PP)	hyperspherical (den. dep. PP)	FN-DMC/ VMC
2	U	S	S
3 (all res.)	U	U	U
3 (two res.)	U	S	U or S(?)GT
4 (all res.)	U	U	U
4 (three res.)	U	S	U <sup>(1)</sup>

but for large  $|a_s|$  deviations are visible. Thus, the system’s behavior is, although qualitatively similar, to some extent non-universal. The three-body energy becomes negative for  $a_s \approx -1.5a_{ho}$  and  $-3a_{ho}$  for the square well and Gaussian potentials, respectively.

The energies for the three-component Fermi system with four atoms per component, i.e., for  $N = 12$ , are shown in Fig. 8 by squares and pluses for the square well and the Gaussian potential, respectively. As in the three-particle case, the energies for these two different potentials agree well for small  $|a_s|$  but behave somewhat differently for large  $|a_s|$ . For both potentials, the  $a_s$  value at which negative energy states appear is similar to that for the corresponding three-body system. An analysis of the structural properties suggests that the  $N = 12$  system is made up of weakly-bound three-body clusters. Figure 8 shows that the energy for  $N = 12$  is larger than four times the energy of the corresponding trimer system, suggesting that the many-body system, which appears to be made up of weakly-bound trimers, may be stable. Our FN-DMC calculations show no evidence for the formation of negative energy states consisting of clusters that contain more than three atoms. At this point it is not clear whether this is a consequence of the particular guiding function employed or whether many-body clusters consisting of four, five or six atoms with negative energy do indeed not exist.

## V. SUMMARY AND CONCLUSION

This paper investigates the stability of trapped  $\chi$ -component Fermi gases interacting through short-range two-body potentials with negative scattering lengths. Table II summarizes the results of our stability analysis.

One of our main findings is that trapped multi-component Fermi gases with more than two components, in which all scattering lengths, masses and trapping fre-

quencies are equal, become unstable for a certain critical negative scattering length. This instability, a type of Fermionova, is similar to the instability of trapped Bose gases with negative scattering length, sometimes referred to as bosonova [25]. The instability predicted here for multi-component Fermi systems,  $\chi > 2$ , emerges within two different theoretical frameworks: A hyperspherical many-body treatment that employs either the bare or a density-dependent zero-range interaction [37, 52], and a many-body Monte Carlo treatment, which includes both VMC and FN-DMC calculation and employs finite-range two-body interactions with a range  $R_0$  chosen so that the first three-particle state with negative energy appears for  $a_s$  much less negative than  $a_c$ .

Both the hyperspherical and the Monte Carlo frameworks parameterize the nodal surface of the anti-symmetric many-body wave function by the ideal gas nodal surface. In the limit of vanishing confinement and periodic boundary conditions, this corresponds to a wave function that describes a normal state. This paper does not investigate wave functions that include pairing physics or the possibility of phase separation from the outset. For three-component systems, for instance, a BCS mean-field framework predicts the existence of a pairing mechanism in which the atoms of species one and two pair (forming a superfluid) while the atoms of species three are in a normal state [30, 32, 33, 35]. This pairing mechanism has also been investigated within other theoretical frameworks [28, 29, 34, 36]. Although the parameter combinations considered in the above cited references is different from those considered in the present paper, we believe that future Monte Carlo studies of multi-component Fermi gases with more than two components should investigate the implications of a many-body wave function that has pairing physics build in from the outset. In particular, it would be interesting to address the question whether a state that contains pairing physics would be stable against the collapse investigated in the present study. If such a stabilizing mechanism existed this would have important consequences for on-going cold atom experiments.

To observe the predicted collapse of multi-component Fermi gases with all-resonant interactions, we imagine the following experiment. First, a stable  $\chi$ -component Fermi gas ( $\chi > 2$ ) with vanishing interspecies scattering lengths is prepared. We then imagine that all interspecies scattering lengths be suddenly tuned to the same large negative value. The time scale for this ramp should be fast compared to the time scale at which phase separation might occur and also fast compared to the time scale at which losses due to spin-flip collisions might occur. The attraction between particles would then produce an implosion and collapse of the system. Following the implosion, we anticipate that recombination into molecules and clusters will immediately follow once the system reaches high density, and the resulting energy release should detonate a fermionova akin to the bosonova that has been observed experimentally and discussed the-

oretically [25, 89, 92, 93, 94, 95]. The rich dynamics of soliton formation, akin to that observed for bosonic atoms in Ref. [96] could also conceivably ensue.

A second main finding of our work concerns three-component Fermi systems with two resonant and one non-resonant interspecies scattering lengths. The behavior of these systems depends strongly on the range  $R_0$  of the underlying two-body potential. For very small  $R_0$ , an instability similar to that for the three-component system with all-resonant interactions appears to arise, although at much more negative  $a_s$ . For larger  $R_0$ , the many-body system may be made up of weakly-bound trimers and may be stable all the way up to unitarity. We note that the importance of the range parameter, or a three-body parameter, was already pointed out in earlier work [31, 35, 36]. Future studies should investigate in more detail whether a Fermi system consisting of weakly- or strongly-bound trimers could be realized experimentally.

Finally, we note that multi-component Fermi gases have recently also been investigated in one-dimensional space [38, 39, 40]. Assuming zero-range interactions, many properties of the multi-component system can be

obtained analytically through the exact Bethe ansatz. For negative coupling constant, the ground state of  $\chi$ -component Fermi gases contains clusters that consist of  $\chi$ -atoms (one of each species). It is suggested that one-dimensional three-component Fermi gases undergo a phase transition that is analogous to the quark color superconductor state [40]. In the future, it would be interesting to investigate whether such a transition also exists in three-dimensional three-component Fermi gases.

Clearly, more work is needed to better understand the behavior of three-dimensional multi-component Fermi gases, including the implications of different two-body ranges and different nodal surfaces of the guiding function employed in the Monte Carlo study. This work investigated the behavior of multi-component Fermi gases for different scattering lengths and two-body ranges. In cases where three-body states with negative energy exist, it will be important to determine if the range of the two-body parameter is indeed the relevant parameter; it may be that the trimer binding energy is a more natural quantity.

We gratefully acknowledge support by the NSF and discussions with J. D’Incao.

- 
- [1] M. H. Anderson, J. R. Ensher, M. R. Matthews, C. E. Wieman, and E. A. Cornell, *Science* **269**, 198 (1995).
  - [2] K. B. Davis, M.-O. Mewes, M. R. Andrews, N. J. van Druten, D. S. Durfee, D. M. Kurn, and W. Ketterle, *Phys. Rev. Lett.* **75**, 3969 (1995).
  - [3] B. DeMarco and D. S. Jin, *Science* **285**, 1703 (1999).
  - [4] M.-O. Mewes, M. R. Andrews, D. M. Kurn, D. S. Durfee, C. G. Townsend, and W. Ketterle, *Phys. Rev. Lett.* **78**, 582 (1997).
  - [5] I. Bloch, T. W. Hänsch, and T. Esslinger, *Phys. Rev. Lett.* **82**, 3008 (1999).
  - [6] E. W. Hagley, L. Deng, M. Kozuma, J. Wen, K. Helmerston, S. L. Rolston, and W. D. Phillips, *Science* **283**, 1706 (1999).
  - [7] M. Greiner, O. Mandel, T. Esslinger, T. W. Hänsch, and I. Bloch, *Nature* **415**, 39 (2002).
  - [8] E. A. Donley, N. R. Claussen, S. T. Thompson, and C. E. Wieman, *Nature* **417**, 529 (2002).
  - [9] W. C. Stwalley, *Phys. Rev. Lett.* **37**, 1628 (1976).
  - [10] E. Tiesinga, B. J. Verhaar, and H. T. C. Stoof, *Phys. Rev. A* **47**, 4114 (1993).
  - [11] S. Inouye, M. R. Andrews, J. Stenger, H. J. Miesner, D. M. Stamper-Kurn, and W. Ketterle, *Nature* **392**, 151 (1998).
  - [12] S. L. Cornish, N. R. Claussen, J. L. Roberts, E. A. Cornell, and C. E. Wieman, *Phys. Rev. Lett.* **85**, 1795 (2000).
  - [13] M. Greiner, C. A. Regal, and D. S. Jin, *Nature* **426**, 537 (2003).
  - [14] M. W. Zwierlein, C. A. Stan, C. H. Schunck, S. M. F. Raupach, S. Gupta, Z. Hadzibabic, and W. Ketterle, *Phys. Rev. Lett.* **91**, 250401 (2003).
  - [15] E. R. I. Abraham, W. I. McAlexander, J. M. Gerton, R. G. Hulet, R. Côté, and A. Dalgarno, *Phys. Rev. A* **55**, 3299(R) (1997).
  - [16] C. A. Regal and D. S. Jin, *Phys. Rev. Lett.* **90**, 230404 (2003).
  - [17] M. Taglieber, A.-C. Vogt, F. Henkel, S. Fray, T. W. Hänsch, and K. Dieckmann, *Phys. Rev. A* **73**, 011402(R) (2006).
  - [18] see, e.g., <http://www.uibk.ac.at/exphys/ultracold/>.
  - [19] G. A. Baker, Jr., *Phys. Rev. C* **60**, 054311 (1999).
  - [20] H. Heiselberg, *Phys. Rev. A* **63**, 043606 (2001).
  - [21] J. Carlson, S. Y. Chang, V. R. Pandharipande, and K. E. Schmidt, *Phys. Rev. Lett.* **91**, 050401 (2003).
  - [22] G. E. Astrakharchik, J. Boronat, J. D. Casulleras, and S. Giorgini, *Phys. Rev. Lett.* **93**, 200404 (2004).
  - [23] In fact, these systems are metastable; however, throughout this paper we call two-component Fermi gases—owing to their long lifetime—stable.
  - [24] R. J. Dodd, M. Edwards, C. J. Williams, C. W. Clark, M. J. Holland, P. A. Ruprecht, and K. Burnett, *Phys. Rev. A* **54**, 661 (1996).
  - [25] E. A. Donley, N. R. Claussen, S. L. Cornish, J. L. Roberts, E. A. Cornell, and C. E. Wieman, *Nature* **412**, 295 (2001).
  - [26] J. L. Roberts, N. R. Claussen, S. L. Cornish, E. A. Donley, E. A. Cornell, and C. E. Wieman, *Phys. Rev. Lett.* **86**, 4211 (2001).
  - [27] A. G. K. Modawi and A. J. Leggett, *J. Low Temp.* **109**, 625 (1997).
  - [28] C. Honerkamp and W. Hofstetter, *Phys. Rev. Lett.* **92**, 170403 (2004).
  - [29] C. Honerkamp and W. Hofstetter, *Phys. Rev. B* **70**, 094521 (2004).
  - [30] L. He, M. Jin, and P. Zhuang, *Phys. Rev. A* **74**, 033604 (2006).
  - [31] A. Sedrakian and J. W. Clark, *Phys. Rev. C* **73**, 035803

- (2006).
- [32] H. Zhai, Phys. Rev. A **75**, 031603(R) (2007).
  - [33] T. Paananen, P. Törmä, and J.-P. Martikainen, Phys. Rev. A **75**, 023622 (2007).
  - [34] R. W. Cherng, G. Refael, and E. Demler, Phys. Rev. Lett. **99**, 130406 (2007).
  - [35] S. Y. Chang and V. R. Pandharipande, physics/0607008v1.
  - [36] P. F. Bedaque and J. P. D’Incao, cond-mat/0602525v2.
  - [37] S. T. Rittenhouse and C. H. Greene, physics/0702161v2.
  - [38] P. Lecheminant, E. Boulat, and P. Azaria, Phys. Rev. Lett. **95**, 240402 (2005).
  - [39] X. W. Guan, M. T. Batchelor, C. Lee, and H.-Q. Zhou, arXiv:0709.1763v1.
  - [40] X.-J. Liu, H. Hu, and P. D. Drummond, arXiv:0709.2273v1.
  - [41] E. Fermi, Nuovo Cimento **11**, 157 (1934).
  - [42] B. D. Esry, Phys. Rev. A **55**, 1147 (1997).
  - [43] S. T. Rittenhouse, M. J. Cavagnero, J. von Stecher, and C. H. Greene, Phys. Rev. A **74**, 053624 (2006).
  - [44] M. E. Gehm, S. L. Hemmer, S. R. Granade, K. M. O’Hara, and J. E. Thomas, Phys. Rev. A **68**, 011401 (2003).
  - [45] H. T. C. Stoof, M. Houbiers, C. A. Sackett, and R. G. Hulet, Phys. Rev. Lett. **76**, 10 (1996).
  - [46] M. Houbiers, R. Ferwerda, H. T. C. Stoof, W. I. McAlexander, C. A. Sackett, and R. G. Hulet, Phys. Rev. A **56**, 4864 (1997).
  - [47] K. E. Strecker, G. B. Partridge, and R. G. Hulet, Phys. Rev. Lett. **91**, 080406 (2003).
  - [48] T. Bourdel, L. Khaykovich, J. Cubizolles, J. Zhang, F. Chevy, M. Teichmann, L. Tarré, S. J. J. M. F. Kokkelmans, and C. Salomon, Phys. Rev. Lett. **93**, 050401 (2004).
  - [49] J. Kinast, S. L. Hemmer, M. E. Gehm, A. Turlapov, and J. E. Thomas, Phys. Rev. Lett. **92**, 150402 (2004).
  - [50] M. Bartenstein, A. Altmeyer, S. Riedl, S. Jochim, C. Chin, J. Hecker Denschlag, and R. Grimm, Phys. Rev. Lett. **92**, 120401 (2004).
  - [51] B. M. Fregoso and G. Baym, Phys. Rev. A **73**, 043616 (2006).
  - [52] J. von Stecher and C. H. Greene, Phys. Rev. A **75**, 022716 (2007).
  - [53] S. Y. Chang, V. R. Pandharipande, J. Carlson, and K. E. Schmidt, Phys. Rev. A **70**, 043602 (2004).
  - [54] D. V. Fedorov and A. S. Jensen, Phys. Rev. A **63**, 063608 (2001).
  - [55] E. Chabanat, P. Bonche, P. B. Haensel, J. Meyer, and R. Schaeffer, Nucl. Phys. A **635**, 231 (1998).
  - [56] S. A. Fayans, S. V. Tolokonnikov, E. L. Trykov, and D. Zawischa, Nucl. Phys. A **676**, 49 (2000).
  - [57] J. L. Bohn, B. D. Esry, and C. H. Greene, Phys. Rev. A **58**, 584 (1998).
  - [58] O. Sørensen, D. V. Fedorov, A. S. Jensen, and E. Nielsen, Phys. Rev. A **65**, 051601 (2002).
  - [59] J. Avery, *Hyperspherical Harmonics: Applications in Quantum Theory* (Kluwer Academic Publishers, Dordrecht, Boston, London, 1989).
  - [60] J. Macek, J. Phys. B **1**, 831 (1968).
  - [61] H. Klar and M. Klar, Phys. Rev. A **17**, 1007 (1978).
  - [62] A. F. Starace and G. L. Webster, Phys. Rev. A **19**, 1629 (1979).
  - [63] C. D. Lin, Phys. Rep. **257**, 1 (1995).
  - [64] F. Werner and Y. Castin, Phys. Rev. A **74**, 053604 (2006).
  - [65] D. Blume, J. von Stecher, and C. H. Greene, Phys. Rev. Lett. **99**, 233201 (2007).
  - [66] J. Carlson and S. Reddy, Phys. Rev. Lett. **95**, 060401 (2005).
  - [67] J. E. Thomas, J. Kinast, and A. Turlapov, Phys. Rev. Lett. **95**, 120402 (2005).
  - [68] J. P. D’Incao and B. D. Esry, Phys. Rev. Lett. **94**, 213201 (2005).
  - [69] F. Werner and Y. Castin, Phys. Rev. Lett. **97**, 150401 (2006).
  - [70] The hyperspherical treatment presented in Ref. [37] uses the value  $\beta = -0.49$  [52] instead of  $\beta = -0.58$ . As a consequence, Ref. [37], predicts that all-resonant three-component systems are stable all the way to unitarity while the present analysis predicts a collapse due to the more negative  $\beta$  value.
  - [71] E. Nielsen and J. H. Macek, Phys. Rev. Lett. **83**, 1566 (1999).
  - [72] E. Nielsen, D. V. Fedorov, A. S. Jensen, and E. Garrido, Phys. Rep. **347**, 374 (2001).
  - [73] L. H. Thomas, Phys. Rev. **47**, 903 (1935).
  - [74] V. Efimov, Phys. Lett. **33B**, 563 (1970).
  - [75] V. Efimov, Yad. Fiz. **12**, 1080 (1970) [Sov. J. Nucl. Phys. **12**, 598 (1971)].
  - [76] V. Efimov, Nucl. Phys. A **210**, 157 (1973).
  - [77] B. L. Hammond, W. A. Lester, Jr., and P. J. Reynolds, *Monte Carlo Methods in Ab Initio Quantum Chemistry* (World Scientific, Singapore, 1994).
  - [78] W. H. Press, S. A. Teukolsky, W. T. Vetterling, and B. P. Flannery, *Numerical Recipes in Fortran, Second Edition* (Cambridge University Press, 1992).
  - [79] N. Metropolis, A. W. Rosenbluth, M. N. Rosenbluth, A. H. Teller, and E. Teller, J. Chem. Phys. **21**, 1087 (1953).
  - [80] R. Jáuregui, R. Paredes, and G. Toledo Sánchez, Phys. Rev. A **76**, 011604(R) (2007).
  - [81] S. Y. Chang and G. F. Bertsch, Phys. Rev. A **76**, 021603(R) (2007).
  - [82] J. von Stecher, C. H. Greene, and D. Blume, Phys. Rev. A **76**, 053613 (2007).
  - [83] P. J. Reynolds, D. M. Ceperley, B. J. Alder, and W. A. Lester, Jr., J. Chem. Phys. **77**, 5593 (1982).
  - [84] This value depends notably on the timestep used in the DMC/FN-DMC calculation.
  - [85] S. Ronen, D. C. E. Bortolotti, D. Blume, and J. L. Bohn, Phys. Rev. A **74**, 033611 (2006).
  - [86] G. E. Astrakharchik, D. Blume, S. Giorgini, and B. E. Granger, J. Phys. B **37**, S205 (2004).
  - [87] H. W. van der Hart, Phys. Rev. A **62**, 013601 (2000).
  - [88] D. Blume and C. H. Greene, Phys. Rev. A **66**, 013601 (2002).
  - [89] V. Pérez-García, H. Michinel, J. I. Cirac, M. Lewenstein, and P. Zoller, Phys. Rev. A **56**, 1424 (1997).
  - [90] H. T. C. Stoof, J. Stat. Phys. **87**, 1353 (1997).
  - [91] J. von Stecher and C. H. Greene, Phys. Rev. Lett. **99**, 090402 (2007).
  - [92] P. A. Ruprecht, M. J. Holland, K. Burnett and M. Edwards, Phys. Rev. A **51**, 4704 (1995).
  - [93] C. C. Bradley and C. A. Sackett and R. G. Hulet, Phys. Rev. Lett. **78**, 985 (1997).
  - [94] C. A. Sackett, J. M. Gerton, M. Welling and R. G. Hulet, Phys. Rev. Lett. **82**, 876 (1999).
  - [95] A. Gammal, T. Frederico and L. Tomio, Phys. Rev. A

- 64**, 055602 (2001).  
[96] S. L. Cornish, S. T. Thompson and C. E. Wieman, Phys. Rev. Lett. **96**, 170401 (2006).